AWARD NUMBER: W81XWH-17-1-0304

TITLE: Validation of Structural, Molecular, and Functional Imaging Biomarkers in Spinal Cord Injury in Non-Human Primates

PRINCIPAL INVESTIGATOR: John C. Gore

CONTRACTING ORGANIZATION: Vanderbilt University Medical Center
Nashville, TN 037232

REPORT DATE: August 2018

TYPE OF REPORT: Annual

PREPARED FOR: U.S. Army Medical Research and Materiel Command
Fort Detrick, Maryland 21702-5012

REPORT DOCUMENTATION PAGE

Form Approved
OMB No. 0704-0188

1. REPORT DATE	2. REPORT TYPE	3. DATES COVERED
August 2018	Annual	15 Jul 2017 - 14 Jul 2018

4. TITLE AND SUBTITLE
Validation of Structural, Molecular, and Functional Imaging Biomarkers in Spinal Cord Injury in Non-Human Primates

5a. CONTRACT NUMBER

5b. GRANT NUMBER
W81XWH-17-1-0304

5c. PROGRAM ELEMENT NUMBER

6. AUTHOR(S)
John C. Gore

Email: john.gore@Vanderbilt.Edu

5d. PROJECT NUMBER

5e. TASK NUMBER

5f. WORK UNIT NUMBER

7. PERFORMING ORGANIZATION NAME(S) AND ADDRESS(ES)
Vanderbilt University Medical Center
Nashville, TN 037232

8. PERFORMING ORGANIZATION REPORT NUMBER

9. SPONSORING / MONITORING AGENCY NAME(S) AND ADDRESS(ES)
U.S. Army Medical Research and Materiel Command
Fort Detrick, Maryland 21702-5012

10. SPONSOR/MONITOR'S ACRONYM(S)

11. SPONSOR/MONITOR'S REPORT NUMBER(S)

12. DISTRIBUTION / AVAILABILITY STATEMENT
Approved for Public Release; Distribution Unlimited

13. SUPPLEMENTARY NOTES

14. ABSTRACT

Spinal cord injuries (SCI) impair sensory, autonomic and/or motor functions, and are a leading cause of disability. The process of spontaneous repair of damaged SC is poorly understood because of a lack of appropriate longitudinal tracking methods. Such a method would provide the information needed for a basic understanding of recovery processes and for determining the optimal time window, targets and effectiveness of therapeutic interventions. Combinations of novel, advanced MRI methods can provide unique insights into SCI progression, especially into the functional integrity of grey matter and micro-structural and biochemical changes in white matter. Much previous work in rodent models has limited significance for human injuries, but studies in non-human primates are directly applicable. We propose to use non-invasive multiparametric MRI at high field to assess changes in structural, functional and cellular/molecular properties of SCI over time in a monkey model and determine how these changes predict and correlate with behavioral recovery.

15. SUBJECT TERMS-

16. SECURITY CLASSIFICATION OF:			17. LIMITATION OF ABSTRACT	18. NUMBER OF PAGES	19a. NAME OF RESPONSIBLE PERSON
a. REPORT	b. ABSTRACT	c. THIS PAGE			USAMRMC
U	U	U	UU	33	19b. TELEPHONE NUMBER *(include area code)*

TABLE OF CONTENTS

1. **INTRODUCTION:** *Narrative that briefly (one paragraph) describes the subject, purpose and scope of the research.*

The research proposed will track longitudinally the spontaneous repair of injured spinal cord in a primate model of cervical spinal cord injury (SCI) using novel, multi-modal MRI methods, and will establish their relationships to gold-standard invasive measures of function and structure in non-human primates. The purpose of the research is to provide the basis for the interpretation of integrated, MRI-based biomarkers for the non-invasive assessment of SCI and repair, which are poorly understood because of a lack of appropriate longitudinal tracking methods. Such information is critical for understanding recovery processes of sensory, autonomic and/or motor functions and for determining the optimal time window, targets, and effectiveness of therapeutic interventions. For the research we will use a combination of advanced MRI methods for provide unique insights into SCI progression, including functional integrity of grey matter and micro-structural and biochemical changes in white matter to assess changes in structural, functional and cellular/molecular properties of SCI over time in a monkey model. We will also determine how these changes predict and correlate with behavioral recovery and histological endpoints, for the development of safe and effective biomarkers for monitoring spinal cord injuries and evaluating treatment outcomes.

2. **KEYWORDS:** *Provide a brief list of keywords (limit to 20 words).*

MRI, fMRI, CEST, qMT, DTI, monkey, spinal cord, cervical

3. **ACCOMPLISHMENTS:** *The PI is reminded that the recipient organization is required to obtain prior written approval from the awarding agency grants official whenever there are significant changes in the project or its direction.*

What were the major goals of the project?

List the major goals of the project as stated in the approved SOW. If the application listed milestones/target dates for important activities or phases of the project, identify these dates and show actual completion dates or the percentage of completion.

Major Goals: Our SOW identified the following major goals for Y1

Major Task 1

(a) Implement high resolution fMRI on NHPs: implement sub-millimeter fMRI at 9.4Tesla along with appropriate acquisition sequences and post-processing algorithms for high quality measures of connectivity in normal animal. *Completed*

(b) Map fMRI evoked responses to touch and heat: Map relevant sensory responses at high resolution to identify candidate seed regions in 3 pre-lesion (normal) animals. *Completed*

(c) Acquire resting state fMRI data in 3 normal NHPs. Quantify fMRI connectivity by seed and data-driven methods : Perform connectivity analyses to identify circuits and degree of connectivity between horns, within and across segments. *Completed*

(d) Implement dorsal column lesion (DCL) injury model in NHPs and acquire MR data at intervals following injury: Image NHPs before and at regular intervals following injury, up to 2 months (first cohort). *50% complete*

(e) Quantify changes in connectivity longitudinally in injured NHPs: Measure connectivity strengths and patterns from fMRI within and across segments at each time point imaged (first cohort). *50% complete*

Milestone 1 for Y1: ACURO approval at 3 mos.
Completion date: September 26, 2017

Milestone 2 for Y1: Completion of first cohort of animals at 9 mos (1a-e).
Completion date (1a-c): July 2, 2018; (1d-e) 50% complete

Major Task 2

(a) Implement high resolution MRI on NHPs: implement sub-millimeter CEST, qMT, and DTI acquisition sequences at 9.4T. *Completed*

(b) Implement appropriate post-processing algorithms to derive parametric maps from CEST, qMT and DTI acquisitions. *Completed*

(c) Implement DCL injury model in NHPs and acquire MR structural and molecular data at intervals following injury: Image NHPs before and at regular intervals following injury, up to 6 month (first cohort). *50% complete*

Milestone for Y1: Completion of first cohort of animals at 9 mos (2a-c).
Completion date (2a-b): June 20, 2018; (2c) 50% complete.

Major Task 3

(a) Validate connectivity from resting state MRI by comparisons with (i) electrophysiology and (ii) histology: Compare high resolution resting state fMRI with electrical recordings and injected tracers to verify functional circuits in spinal cord of squirrel monkeys. *50% complete.*

(b) Perform electrophysiologic recordings from spinal cords of NHPs post SCI at specific time points: Implement surface and microelectrode recordings and measure inter-regional synchrony and coherence (first cohort). *50% complete.*

(c) Verify injury locations and nature using histology: Perform post-mortem histological studies with appropriate stains (cytochrome oxidase, Nissl, Myelin, VGluT2) at specific time points and at end of 6 months. *50% complete.*

Milestone for Y1: Completion of first cohort of animals at 9 mos (3a-c).
(*3a-c) 50% complete.*

What was accomplished under these goals?

For this reporting period describe: 1) major activities; 2) specific objectives; 3) significant results or key outcomes, including major findings, developments, or conclusions (both positive and negative); and/or 4) other achievements. Include a discussion of stated goals not met. Description shall include pertinent data and graphs in sufficient detail to explain any significant results achieved. A succinct description of the methodology used shall be provided. As the project progresses to completion, the emphasis in reporting in this section should shift from reporting activities to reporting accomplishments.

1) Major activities included (1a) implementation of high resolution, sub-millimeter functional MRI in NHPs at 9.4 Tesla; (1b) ACURO approval; (2) implementation of high resolution MRI on NHP at 9.4T for sub-millimeter CEST, qMT, and DTI acquisitions in NHP; and (3) validation of fMRI resting state (rs) connectivity by comparisons with electrophysiology and histology of injected tracers to verify functional circuits in spinal cord in the first cohort of SCI monkeys.

Specifically, for (1a) fMRI, appropriate acquisition sequences and post-processing algorithms for measuring connectivity were applied in normal animals for mapping fMRI evoked responses to touch and heat to identify candidate seed regions for acquiring resting state fMRI data. These data were analyzed to quantify resting state connectivity by seed and independent component analysis (ICA) methods to identify circuits and degrees of connectivity between horns, within and across segments. The implementation of the DCL injury model in the first cohort of NHPs and the acquisition of MR data at regular intervals following injury, up to 2 months, commenced to begin the quantification of changes in connectivity longitudinally in injured NHPs including fMRI connectivity strengths and patterns within and across segments at each time point imaged. For (2) CEST, qMT, and DTI acquisition sequences at 9.4T, and appropriate post-processing algorithms to derive parametric maps, were implemented. The DCL injury model in the first cohort of NHPs was initiated to begin the acquisition of MR structural and molecular data at regular intervals following injury, for up to 2 months. For (3) validation of fMRI resting state connectivity by comparisons with electrophysiology, we have implemented surface and electrode array recordings of NHP spinal cord post SCI at specific time points and measured inter-regional synchrony and coherence in the first monkey cohort. Verification of injury location and nature using histology with appropriate stains (cytochrome oxidase, Nissl, Myelin, VGluT2) at specific time points and at end of 2 months has commenced. Behavioral training of monkeys has also begun.

2) Specific Objectives

(1) Determine how the functional integrity of injured spinal cord grey matter repairs over time using functional MRI.

(2) Determine how injured spinal cord white matter repairs over time using structural and molecular MRI.

(3) Validate our MRI findings with invasive, gold-standard measures. These will include electrophysiology, behavioral measures, and quantitative analyses of histological sections obtained at different time points during the course of recovery.

3) Significant results

Functional MRI data are critical for quantifying the functional integrity of the nervous system, including the spinal cord. However, the fMRI signal changes need to be interpreted in order to understand how injured spinal cord grey matter repairs over time. Spinal cord fMRI data were acquired at 9.4T using a 4-shot segmented echo planar imaging sequence in anesthetized, mechanically ventilated monkeys with a saddle-shaped transmit-receive surface coil positioned over the neck. We measured the BOLD signal change (Fig. 1F) and mapped fMRI evoked responses to tactile stimuli in normal animals (Fig. 1G). We also identified resting state connectivity patterns with significant correlations to the seed (Fig 1H).

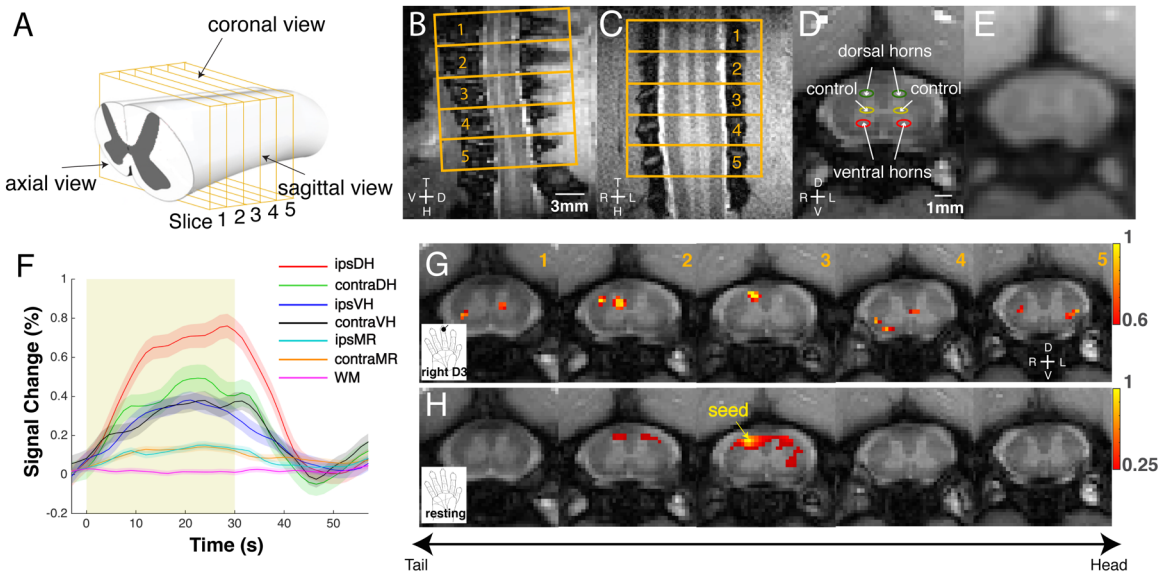

Figure 1: Stimulus-driven and resting-state fMRI in non-human primates at 9.4T. (A) Schematic diagram of imaging planes of the spinal cord. (B) Sagittal and (C) coronal views of the spinal cord in magnetization transfer contrast (MTC) images. (D) MTC and (E) BOLD sensitive axial images. Red and green circles indicate dorsal and ventral horns respectively. Yellow circles present intermediate gray matter of the spinal cord used as controls for later quantifications. (F) Group averaged (N=7 monkeys) BOLD signal changes in the four horns – dorsal horn (DH) and ventral horn (VH) – of the spinal cord and middle/intermediate gray matter regions (MR) that are ipsilateral (ipsi) and contralateral (contra) to the stimulus, as well as white matter (WM) control region. (G) Multi-run activation map to D3 tactile stimulation thresholded at 0.6 of normalized percentage signal, with a peak value of 1. (H) Multi-run resting-state connectivity patterns (thresholded at r>0.25) of seed from one representative monkey. D, dorsal; V, ventral; H, head; T, tail.

We validated fMRI resting state connectivity by comparisons with electrophysiologic recordings from spinal cords of NHPs to measure inter-regional synchrony and coherence. Single epoxylite-coated tungsten microelectrode (~1MΩ impedance) with standard exposed sharp tip (< 3μm) were used for mapping the spinal cord. Penetration depths of each microelectrode were recorded and performed at 300μm increments. At each interval, hand digits of the animals were tapped lightly while receptive field of neurons were characterized.

Neuronal responses to tactile stimuli were recorded and analyzed (Fig. 2, LFP, MUA).

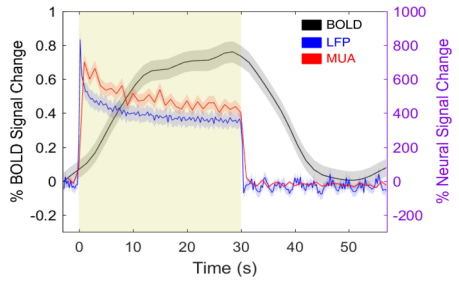

Figure 2: Responses to innocuous tactile stimulation of digits in the spinal cord. Overlay of averaged time courses of fMRI (black), LFP (blue) and MUA (red) responses in the ipsilateral dorsal horn. Shaded yellow region represents stimulus-on period. LFP signals are represented with computed r.m.s. (bin size=0.25s, no overlap, N=4 monkeys, n= 40 runs) while MUA are presented as spike rates (bin size=1s, no overlap, N=2 monkeys, n=24 runs). Percentage signal changes for BOLD and neural signal were computed relative to pre-stimulus period; BOLD and electrophysiological signals are plotted against y-scale on the left (black) and right (purple) respectively. (The signals from the two modalities were not acquired simultaneously.)

For connectivity, within-slice dorsal-dorsal functional connectivity was observed to be stronger (mean BOLD r=0.49 and LFP coherence=0.19) than that in the dorsal gray-commissure (averaged between left and right BOLD r=0.40 and LFP coherence=0.12) for both fMRI and LFP (Fig. 3B-C). Moreover, LFP dorsal-dorsal coherence was found to be statistically significant at depths up to 1.5 mm for correlations of contralateral regions at precisely the same depth. While within-slice resting-state connectivity was robust between horns, across-slice correlation strengths were consistently lower (mean BOLD r=0.26 and LFP coherence=0.03).

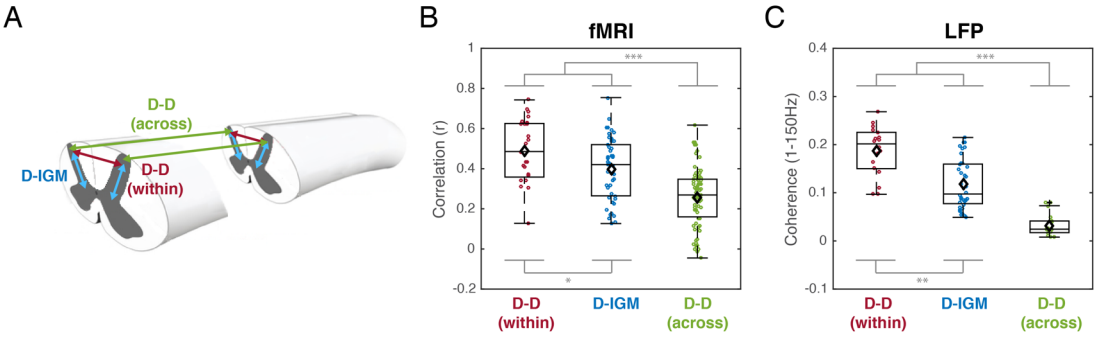

Figure 3: Comparison between resting-state fMRI and LFP connectivities. (A) Schematic diagram of correlation and coherences computed in spinal cord recordings. (B,C) Group averaged within and across segments dorsal to dorsal (D-D) and dorsal to intermediate GM (D-IGM) connectivity. Group boxplots of connectivity measures are displayed as Pearson's correlation for fMRI and averaged coherences for LFP. Each boxplot contains fMRI observations (n=25, 50 and 75) from eleven monkeys (a subset was from this project) (B) and electrophysiology observations (n=18, 36 and 18) from four monkey studies (C). The median and mean of are represented as horizontal lines and diamonds respectively in each boxplot. Scatter circles on each boxplot represent individual observations. *p<0.05, **p<0.0005, and ***p<0.00005 Bonferroni-Holm corrected 2-sided Mann-Whitney test.

Resting state fMRI was applied to monkeys pre- and post-lesion to determine changes in connectivity within the spinal cord. Significant differences in functional connectivity were observed post-lesion between specific horn connections (Fig. 4). Functional connectivity decreased between left and right dorsal horn and left and dorsal and left ventral horns (Fig. 4).

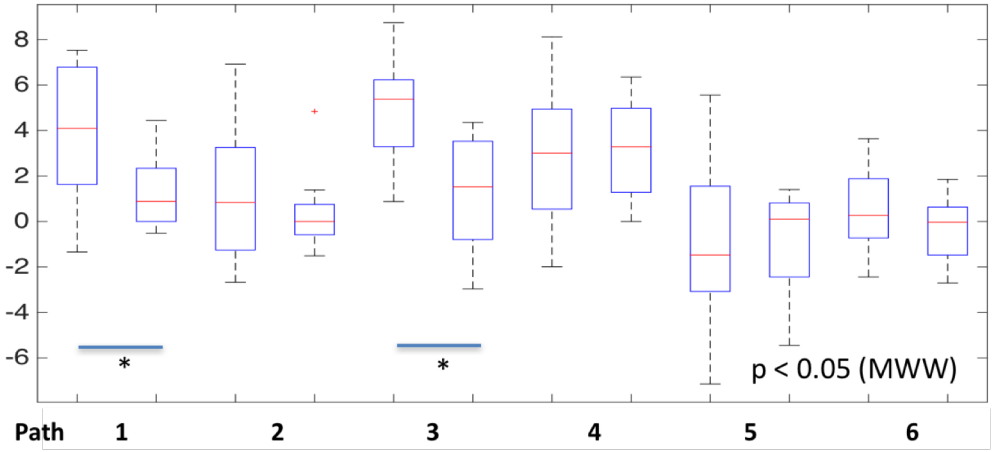

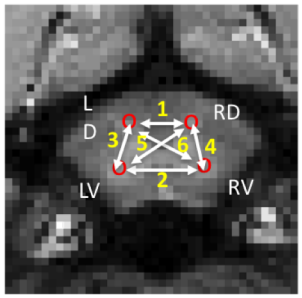

1. Left Dorsal - Right Dorsal (LD-RD)
2. Left Ventral - Right Ventral (LV-RV)
3. Left Dorsal - Left Ventral (LD-LV)
4. Right Dorsal - Right Ventral (RD-RV)
5. Left Dorsal - Right Ventral (LD-RV)
6. Right Dorsal - Left Ventral (RD-LV)

Figure 4: Effects of a unilateral dorsal column lesion on interslice ROI connectivity in a representative monkey. Top: Whisker box plots of functional connectivities (Z-scores) between horn ROI pairs (1-6). Error bars indicated the standard deviation of the measurements. *p<0.05. Data sets represent twelve runs before and after spinal cord lesion (2 weeks post lesion). Preprocessing included muscle and cerebral spinal fluid regression.

In summary, for fMRI and its validation with electrophysiology, (1) both BOLD and electrophysiologic signals elicited by tactile stimulation occurred predominantly in the ipsilateral dorsal horn and only in digit-appropriate segments; (2) resting-state dorsal-dorsal functional connectivity is significantly greater than that of dorsal-to-intermediate-gray-matter in both modalities; (3) resting-state functional connectivity is strongest within its own segment; (4) there was high concordance between LFP and fMRI metrics; and (5) injury reduces functional connectivities within a spine segment.

Structural and microstructural changes occur after spinal cord injury, including molecular changes and structural (white matter) injury. To measure these *in vivo* in monkeys, CEST, qMT, and DTI data were acquired at 9.4T in the DCL injury model at regular intervals following injury.

CEST imaging was performed to obtain Z-spectra using a continuous wave (4.0 s, 1.0 μT) irradiation pulse followed by a 2-shot SE-EPI readout (with TR 6.0 s, TE 17.6 ms) in three monkeys and they were scanned at different time points for up to 24 weeks after the injury. an anatomic image and the correlation map of the Z- spectra in an injured spinal cord. Compared to normal GM, amide, amine and hydroxyl CEST effects were strong while the semisolid magnetization transfer (MT) and nuclear Overhauser enhancement (NOE) effects were weak in regions identified as cystic. In addition, higher peak amplitudes and narrower widths were observed for the large component of free water in cysts. Abnormal tissues around the lesion site also showed different Z-spectra compared to those of cysts and normal tissues. Different spectra were observed for normal tissue, scar tissue, abnormal tissue rostral or caudal to the lesion, and cysts. Longitudinally, all subjects exhibited recovery from SCI with the shrinkage of, reduction of CEST effects, and increments of semisolid MT and NOE effects at or around the lesion site (data not shown).

Quantitative MT MRI provides a noninvasive means to detect and grade myelination after an injury and during repair. qMT data were collected at 9.4T using a 2D MT-weighted spoiled gradient recalled-echo sequence for a coronal slice before and after a unilateral dorsal column lesion of the cervical spinal cord. MTC can detect lesions in the spinal cord (Fig. 6).

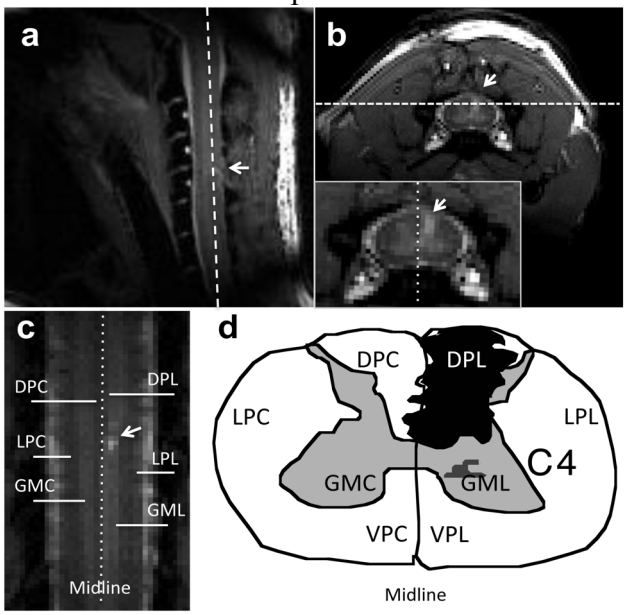

Figure 6. **MTC images showing a unilateral dorsal column lesion in squirrel monkey**. (a) Sagittal view. (b) Axial view. (c) Coronal view. (d) Schematic illustration of the targeted lesion of unilateral dorsal column (black patch). The arrow indicates the lesion site. White dashed lines indicate the location of a coronal imaging plan. DPC, LPC, VPC and GMC indicate dorsal pathway, lateral pathway, ventral pathway and gray matter (GM) on the control side respectively; DPL, LPL, VPL and GML indicate dorsal pathway, lateral pathway, ventral pathway and GM on the lesion side respectively.

We systematically evaluated the accuracy and precision of estimates of pool size ratio (PSR) from qMT using different modeling approaches with a main goal of optimizing a rapid, sensitive and high-resolution PSR mapping protocol for assessing SCI in primates at high field. All of the selected modeling approaches, using either 5-, 2- or 1-parameter modeling, were able to detect the lesion as a change in PSR at the site of injury (Fig. 7).

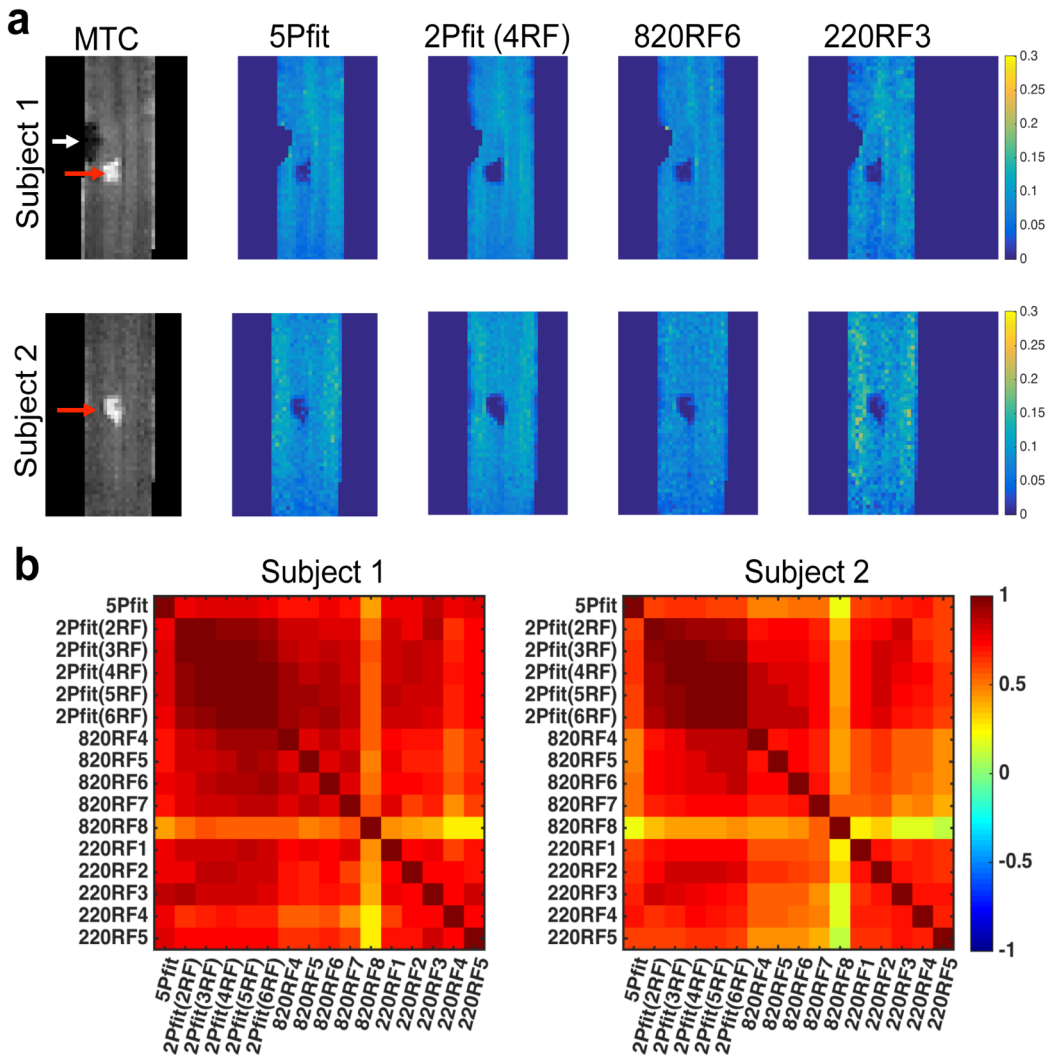

Figure 7. **Comparison of PSR of injured spinal cord of squirrel monkey from different modeling approaches**. (a) Selected PSR maps showing 5-parameter fitting (5Pfit) using data with 12 RF offsets, 2-parameter fitting (2Pfit) using data with 4 RF offsets, 1-parameter calculation based on data with RF6 and RF12 at 820° (820RF6), and 1-parameter calculation based on data with RF3 and RF12 at 220° (220RF3). (b) Correlation coefficients between PSR measures from selected modeling approaches ($p < 0.05$ for all). All pixels in the middle 1.5 cm were included in the correlation analysis.

Histology confirmed that reduced PSR values correspond to demyelination along the dorsal pathway on the injury side (Fig. 8). The side rostral to the lesion showed more severe demyelination than the caudal side in the injured subjects (Fig. 8).

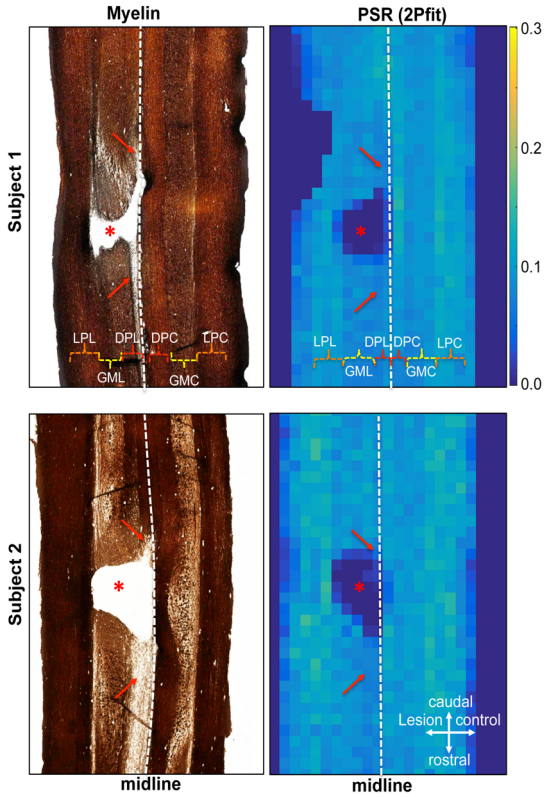

Figure 8. **Comparison of PSR maps and corresponding spinal cord tissue with myelin staining.** Asterisks indicate lesions/cysts, and red arrows indicate unilateral demyelination in the dorsal pathway on the lesion side, both caudal and rostral to the lesion site. PSR maps from 2-parameter fitting using 4 RF offsets are shown for comparison. DPC, LPC, and GMC indicate dorsal pathway, lateral pathway, and GM on the control side respectively; DPL, LPL, and GML indicate dorsal pathway, lateral pathway, and GM on the lesion side respectively.

The optimum 2- and 1-parameter approaches were very sensitive in detecting cysts (Fig. 9), and they also provided comparable sensitivity as 5-parameter modeling to detect regional demyelination and loss of macromolecules around the injury site (Fig. 9). The decrease of PSR in GM (Fig. 9) was not as evident as that in the dorsal pathway. The results from 2- or 1-parameter modeling could underestimate PSR of cyst (Fig. 9), due to the relative bias caused by fixing R_aT_{2a}, T_{2b}, and RM_{0a} when their actual values are very different in cyst.

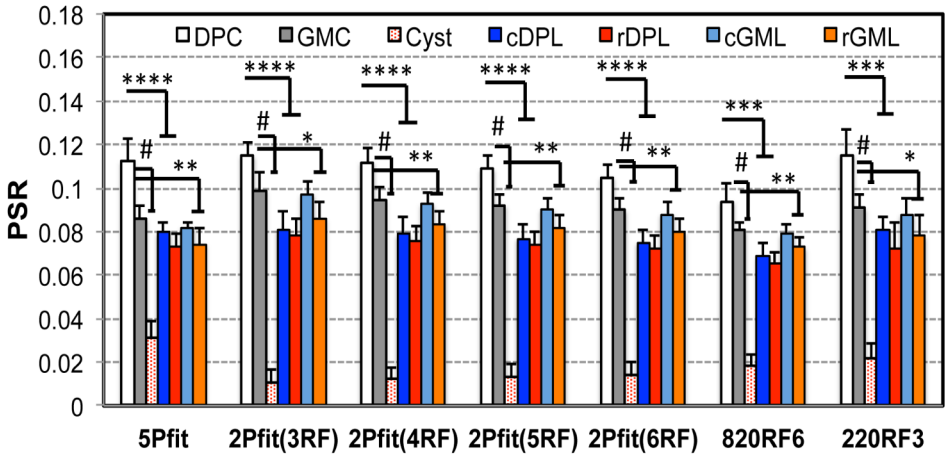

Figure 9. Comparison of regional PSR of injured spinal cord across subjects. (a) The regional averaged PSR across subjects from selected modeling approaches. Bars represent standard deviations. DPC and GMC indicate the dorsal pathway and GM on the control, while rDPL, cDPL, rGML, and cGML indicate rostral dorsal pathway, caudal dorsal pathway, rostral GM, and caudal GM on the lesion side of the injured subjects, respectively. (N=12 control, N=5 injured)

In summary, the qMT results support the use of the optimized 2- or 1-parameter approach for qMT imaging of injured spinal cord as a means to reduce total imaging time and/or allow additional signal averaging. PSR could detect demyelination rostral and caudal to lesions, especially in the dorsal pathway on the lesion side.

Diffusion tensor imaging (DTI) was used to quantify changes in the dorsal and lateral white matter pathways in the cervical spinal cord of squirrel monkeys before and after injury. For DTI, a respiratory-gated, spin-echo echo-planar imaging protocol was implemented (TR/TE = 3000/35ms; duration of gradient pulse/diffusion time (δ/Δ = 4/12 ms); amplitude = 19.96 gauss/cm; b-value (1000 s/mm^2); 30 gradient directions; isotropic spatial resolution 0.5×0.5×0.5mm^3; matrix size 64×64×8; sampling band width 250 kHz; number of excitation 16). A diffusion tensor was derived for each voxel using the thirty diffusion-weighted acquisitions from different orientations using CAMINO. We calculated the fractional anisotropy (FA), mean diffusivity (MD), and axial and radial diffusivities (AD, RD).
Figure 10 shows representative axial diffusivity (AD), fractional anisotropy (FA), mean diffusivity (MD) and radial diffusivity (RD) maps from DTI after spinal cord injury.

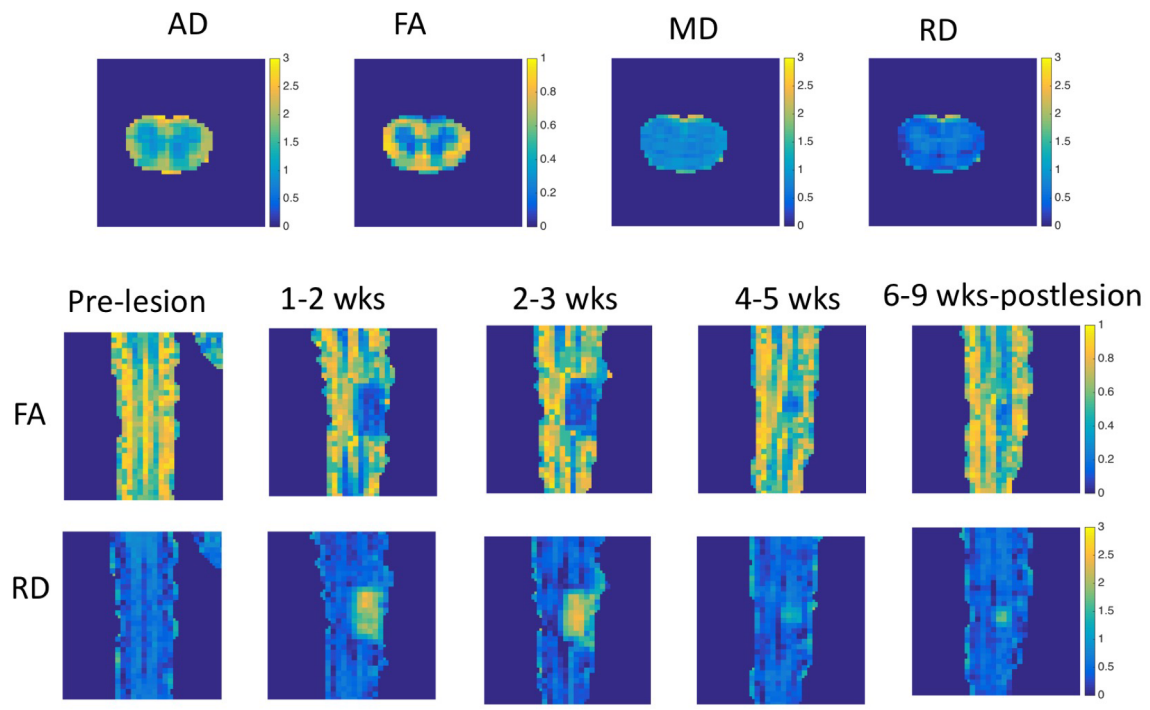

Figure 10. Longitudinal evaluation of the axonal integrity in one representative monkey. Top row: axial AD, FA, MD and RD maps of one slice at 19 days post-injury time point. Bottom two rows: repeated FA and RD maps at pre- and different time points post lesion. Figure 10A-D shows the linearly interpolated FA, MD, AD and RD maps overlaid on the MTC image (a pink arrow points to the lesion). Diffusion parameters were observed to be significantly larger at the lesion site in comparison to the white and gray matter pathways.

DTI parameters were quantified and compared pre- and post-injury (Figure 12). The whisker boxplot in Figure 11A-D shows the distribution of values of four diffusion parameters before injury and over the recovery period. Statistical significance of the difference between measured parameters (pre- and post-injury) at a stage of recovery (5-weeks) was measured using a pair wise non-parametric rank-sum test (Mann Whitney Wilcoxon test, MWW). A p value (< 0.05, 0.005) was considered statistically significant in the analysis. FA and RD were significantly different pre-lesion versus the post-lesion stage. However, there were no significant differences in MD or AD pre- versus post-injury.

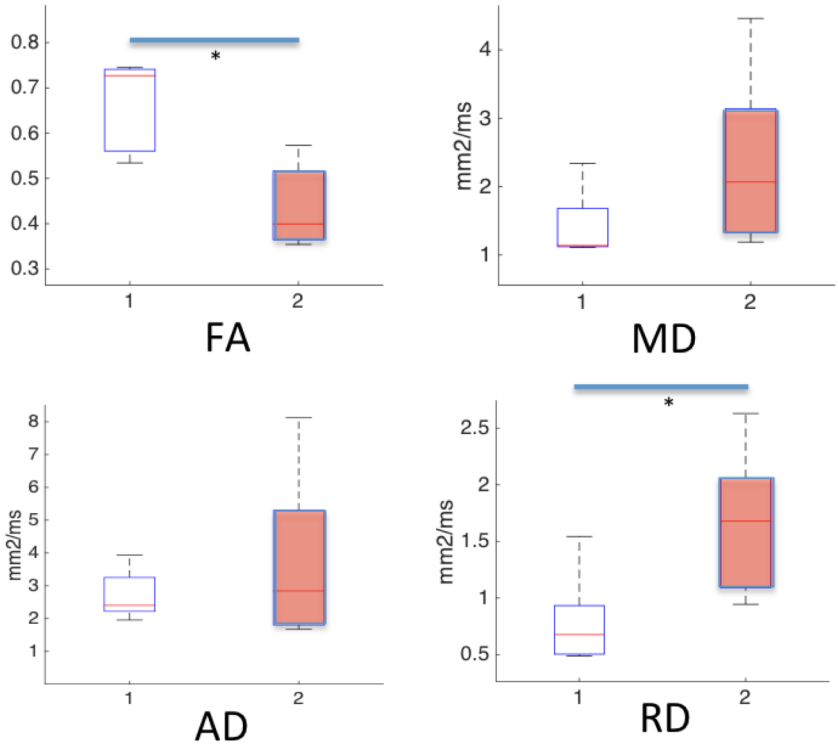

Figure 12. Pre- and post- SCI diffusion parametric changes over the 5-week recovery period. Whisker boxplots show the time courses of the FA (fractional anisotropy), MD (mean diffusivity), AD (axial diffusivity), and RD (radial diffusivity) parametric changes at the pre-lesion, followed by post-lesion stage. The (*) represents p (<0.05) value of statistical significance of difference using MWW test.

Overall, BOLD and resting-state connectivity fMRI results validated with electrophysiology suggest that rs fMRI signals acquired at high field directly reflect underlying neuronal activity at rest and during processing of an external stimuli. CEST, qMT, and DTI were also sensitive to changes in injury and recovery. For DTI, specifically, changes in FA and radial diffusivity over the recovery period demonstrates that there is statistically significant difference between lesioned dorsal column and lateral pathways are sensitive to injury and recovery.

What opportunities for training and professional development has the project provided?
If the project was not intended to provide training and professional development opportunities or there is nothing significant to report during this reporting period, state "Nothing to Report."

Describe opportunities for training and professional development provided to anyone who worked on the project or anyone who was involved in the activities supported by the project. "Training" activities are those in which individuals with advanced professional skills and experience assist others in attaining greater proficiency. Training activities may include, for example, courses or one-on-one work with a mentor. "Professional development" activities result in increased knowledge or skill in one's area of expertise and may include workshops, conferences, seminars, study groups, and individual study. Include participation in conferences, workshops, and seminars not listed under major activities.

The project provided training opportunities for a Biomedical Engineering graduate student in fMRI and electrophysiological methodologies and analyses and professional development for an Instructor through conference participation.

How were the results disseminated to communities of interest?
If there is nothing significant to report during this reporting period, state "Nothing to Report."

Describe how the results were disseminated to communities of interest. Include any outreach activities that were undertaken to reach members of communities who are not usually aware of these project activities, for the purpose of enhancing public understanding and increasing interest in learning and careers in science, technology, and the humanities.

Nothing to Report.

What do you plan to do during the next reporting period to accomplish the goals?
If this is the final report, state "Nothing to Report."

Describe briefly what you plan to do during the next reporting period to accomplish the goals and objectives.

We will perform the studies as outlined in the SOW milestones. This includes (a) implementing the DCL injury model in NHPs and acquire MR data before and at regular intervals following SCI, for additional cohorts; (b) quantifying changes in functional connectivity longitudinally in injured NHPs in additional cohorts; (c) implementing high resolution CEST, qMT, and DTI in the DCL injury model in NHPs in additional cohorts; and (d) validating connectivity from resting state MRI by comparisons with electrophysiology, behavior, and histology. We plan to report our findings at conferences, in journal articles, and presentations.

4. **IMPACT:** D*escribe distinctive contributions, major accomplishments, innovations, successes, or any change in practice or behavior that has come about as a result of the project relative to:*

What was the impact on the development of the principal discipline(s) of the project?
If there is nothing significant to report during this reporting period, state "Nothing to Report."

Describe how findings, results, techniques that were developed or extended, or other products from the project made an impact or are likely to make an impact on the base of knowledge, theory, and research in the principal disciplinary field(s) of the project. Summarize using language that an intelligent lay audience can understand (Scientific American style).

Nothing to Report.

What was the impact on other disciplines?
If there is nothing significant to report during this reporting period, state "Nothing to Report."

Describe how the findings, results, or techniques that were developed or improved, or other products from the project made an impact or are likely to make an impact on other disciplines.

Nothing to Report.

What was the impact on technology transfer?
If there is nothing significant to report during this reporting period, state "Nothing to Report."

Describe ways in which the project made an impact, or is likely to make an impact, on commercial technology or public use, including:

- *transfer of results to entities in government or industry;*
- *instances where the research has led to the initiation of a start-up company; or*
- *adoption of new practices.*

Nothing to Report.

What was the impact on society beyond science and technology?
If there is nothing significant to report during this reporting period, state "Nothing to Report."

Describe how results from the project made an impact, or are likely to make an impact, beyond the bounds of science, engineering, and the academic world on areas such as:

- *improving public knowledge, attitudes, skills, and abilities;*
- *changing behavior, practices, decision making, policies (including regulatory policies), or social actions; or*
- *improving social, economic, civic, or environmental conditions.*

Nothing to Report.

5. CHANGES/PROBLEMS: *The PD/PI is reminded that the recipient organization is required to obtain prior written approval from the awarding agency grants official whenever there are significant changes in the project or its direction. If not previously reported in writing, provide the following additional information or state, "Nothing to Report," if applicable:*

Changes in approach and reasons for change
Describe any changes in approach during the reporting period and reasons for these changes. Remember that significant changes in objectives and scope require prior approval of the agency.

Nothing to Report.

Actual or anticipated problems or delays and actions or plans to resolve them
Describe problems or delays encountered during the reporting period and actions or plans to resolve them.

There was a delay in IACUC approval by the local agency, but after the final protocol approval on September 26, 2017, four monkeys were purchased, and experiments commenced after an 8-week quarantine period. During this time, we imaged phantoms to refine the MRI data acquisition to obtain adequate signal to noise and spatial resolution for each type of acquisition and appropriate post-processing algorithms. We will complete an additional 3 monkeys to complete Year 1 milestones that are 50% complete (we are behind schedule because of delayed IACUC approval).

Changes that had a significant impact on expenditures

Describe changes during the reporting period that may have had a significant impact on expenditures, for example, delays in hiring staff or favorable developments that enable meeting objectives at less cost than anticipated.

None

Significant changes in use or care of human subjects, vertebrate animals, biohazards, and/or select agents

Describe significant deviations, unexpected outcomes, or changes in approved protocols for the use or care of human subjects, vertebrate animals, biohazards, and/or select agents during the reporting period. If required, were these changes approved by the applicable institution committee (or equivalent) and reported to the agency? Also specify the applicable Institutional Review Board/Institutional Animal Care and Use Committee approval dates.

Significant changes in use or care of human subjects

Not applicable.

Significant changes in use or care of vertebrate animals

None

Significant changes in use of biohazards and/or select agents

None

6. **PRODUCTS:** *List any products resulting from the project during the reporting period. If there is nothing to report under a particular item, state "Nothing to Report."*

- **Publications, conference papers, and presentations**
  Report only the major publication(s) resulting from the work under this award.

  Journal publications. *List peer-reviewed articles or papers appearing in scientific, technical, or professional journals. Identify for each publication: Author(s); title; journal; volume: year; page numbers; status of publication (published; accepted, awaiting publication; submitted, under review; other); acknowledgement of federal support (yes/no).*

Nothing to Report.

  Books or other non-periodical, one-time publications. *Report any book, monograph, dissertation, abstract, or the like published as or in a separate publication, rather than a periodical or series. Include any significant publication in the proceedings of a one-time conference or in the report of a one-time study, commission, or the like. Identify for each one-time publication: author(s); title; editor; title of collection, if applicable; bibliographic information; year; type of publication (e.g., book, thesis or dissertation); status of publication (published; accepted, awaiting publication; submitted, under review; other); acknowledgement of federal support (yes/no).*

Nothing to Report.

  Other publications, conference papers and presentations. *Identify any other publications, conference papers and/or presentations not reported above. Specify the status of the publication as noted above. List presentations made during the last year (international, national, local societies, military meetings, etc.). Use an asterisk (*) if presentation produced a manuscript.*

Conference Proceedings: 1. Tung-Lin Wu, Pai-Feng Yang, Feng Wang, Zhaoyue Shi, Arabinda Mishra, Ruiqi Wu, Li Min Chen, John Gore. Validation of spinal cord fMRI with LFP and spike activity in non-human primates. Proc Intl Soc Mag Reson Med 2018. 2. Feng Wang, Tung-Lin Wu, Ke Li, Li Min Chen, John C. Gore (2018). Rapid and robust high-resolution mapping of proton pool size ratio in spinal cord after injury in squirrel monkeys. Proc. Int. Soc.Magn. Reson. Med. 2018.

- **Website(s) or other Internet site(s)**

List the URL for any Internet site(s) that disseminates the results of the research activities. A short description of each site should be provided. It is not necessary to include the publications already specified above in this section.

Nothing to Report.

- **Technologies or techniques**
  Identify technologies or techniques that resulted from the research activities. Describe the technologies or techniques were shared.

Nothing to Report.

- **Inventions, patent applications, and/or licenses**
  Identify inventions, patent applications with date, and/or licenses that have resulted from the research. Submission of this information as part of an interim research performance progress report is not a substitute for any other invention reporting required under the terms and conditions of an award.

Nothing to Report.

- **Other Products**
  Identify any other reportable outcomes that were developed under this project. Reportable outcomes are defined as a research result that is or relates to a product, scientific advance, or research tool that makes a meaningful contribution toward the understanding, prevention, diagnosis, prognosis, treatment and /or rehabilitation of a disease, injury or condition, or to improve the quality of life. Examples include:
  - *data or databases;*
  - *physical collections;*
  - *audio or video products;*
  - *software;*
  - *models;*
  - *educational aids or curricula;*
  - *instruments or equipment;*
  - *research material (e.g., Germplasm; cell lines, DNA probes, animal models);*
  - *clinical interventions;*
  - *new business creation; and*

Nothing to Report.

7. PARTICIPANTS & OTHER COLLABORATING ORGANIZATIONS

What individuals have worked on the project?

Provide the following information for: (1) PDs/PIs; and (2) each person who has worked at least one person month per year on the project during the reporting period, regardless of the source of compensation (a person month equals approximately 160 hours of effort). If information is unchanged from a previous submission, provide the name only and indicate "no change".

Name: Nellie Byun
Project Role: Program Manager
Researcher Identifier (e.g. ORCID ID): 0000-0003-3351-7375
Nearest person month worked: 3
Contribution to Project: Dr. Byun has refined and updated animal protocols, assisted in performing electrophysiology research, coordinated activities between the lab and Division of Animal Care (orders, facility transfers), and purchased lab supplies.

Name: Limin Chen
Project Role: Co-Investigator
Researcher Identifier (e.g. ORCID ID): 0000-0001-9662-1925
Nearest person month worked: 2
Contribution to Project: Dr. Chen has worked on refining the animal care protocol, participated in the optimization MRI data acquisition protocols and electrophysiology, and worked with vendor and DAC at Vanderbilt on new animal purchases.

Name: John Gore
Project Role: Principal Investigator
Researcher Identifier (e.g. ORCID ID): 0000-0002-9480-0900
Nearest person month worked: 1
Contribution to Project: Dr. Gore has arranged and supervised all the experiments, optimizations, and analyses performed.

Name: Feng Wang
Project Role: Co-Investigator
Researcher Identifier (e.g. ORCID ID):
Nearest person month worked: 2
Contribution to Project: Dr. Wang has optimized the MRI data acquisition protocol, refined the data analysis pipeline, and performed MRI experiments

Name: George H. Wilson
Project Role: (Former) Program Manager
Researcher Identifier (e.g. ORCID ID): 0000-0002-1246-6313
Nearest person month worked: 1
Contribution to Project: Mr. Wilson has performed a research assistant role, assisting animal protocol developments, preparation of electrophysiological recordings, and purchasing lab supplies

Name: Pai-Feng Yang
Project Role: Co-Investigator
Researcher Identifier (e.g. ORCID ID): 0000-0003-0265-4772
Nearest person month worked: 3
Contribution to Project: Dr. Yang has optimized in vivo multi-channel micro-electrode electrophysiological recording protocol, refined data preprocessing and analysis pipelines, and performed electrophysiology experiments.

Has there been a change in the active other support of the PD/PI(s) or senior/key personnel since the last reporting period?
If there is nothing significant to report during this reporting period, state "Nothing to Report."

If the active support has changed for the PD/PI(s) or senior/key personnel, then describe what the change has been. Changes may occur, for example, if a previously active grant has closed and/or if a previously pending grant is now active. Annotate this information so it is clear what has changed from the previous submission. Submission of other support information is not necessary for pending changes or for changes in the level of effort for active support reported previously. The awarding agency may require prior written approval if a change in active other support significantly impacts the effort on the project that is the subject of the project report.

Nothing to Report.

What other organizations were involved as partners?
If there is nothing significant to report during this reporting period, state "Nothing to Report."

Describe partner organizations – academic institutions, other nonprofits, industrial or commercial firms, state or local governments, schools or school systems, or other organizations (foreign or domestic) – that were involved with the project. Partner organizations may have provided financial or in-kind support, supplied facilities or equipment, collaborated in the research, exchanged personnel, or otherwise contributed.

Provide the following information for each partnership:
Organization Name:
Location of Organization: (if foreign location list country)
Partner's contribution to the project (identify one or more)

- *Financial support;*
- *In-kind support (e.g., partner makes software, computers, equipment, etc., available to project staff);*
- *Facilities (e.g., project staff use the partner's facilities for project activities);*
- *Collaboration (e.g., partner's staff work with project staff on the project);*
- *Personnel exchanges (e.g., project staff and/or partner's staff use each other's facilities, work at each other's site); and*
- *Other.*

Nothing to Report.

8. SPECIAL REPORTING REQUIREMENTS

COLLABORATIVE AWARDS: *For collaborative awards, independent reports are required from BOTH the Initiating Principal Investigator (PI) and the Collaborating/Partnering PI. A duplicative report is acceptable; however, tasks shall be clearly marked with the responsible PI and research site. A report shall be submitted to* ***https://ers.amedd.army.mil*** *for each unique award.*

Not applicable.

QUAD CHARTS: *If applicable, the Quad Chart (available on https://www.usamraa.army.mil) should be updated and submitted with attachments.*

Submitted with report.

9. APPENDICES: *Attach all appendices that contain information that supplements, clarifies or supports the text. Examples include original copies of journal articles, reprints of manuscripts and abstracts, a curriculum vitae, patent applications, study questionnaires, and surveys, etc.*

See attached.

3669

Rapid and robust high-resolution mapping of proton pool size ratio in spinal cord after injury in squirrel monkeys

Feng Wang[1,2], Tung-Lin Wu[1,3], Ke Li[1], Li Min Chen[1,2], and John C. Gore[1,2,3]

[1]Institute of Imaging Science, Vanderbilt University Medical Center, Nashville, TN, United States, [2]Department of Radiology and Radiological Sciences, Vanderbilt University Medical Center, Nashville, TN, United States, [3]Department of Biomedical Engineering, Vanderbilt University, Nashville, TN, United States

Synopsis

High-resolution quantitative magnetization transfer (qMT) MRI provides a noninvasive means to detect and characterize myelination before and after neural injury and during repair. This study aims to systematically evaluate the accuracy and precision of pool size ratio (PSR) measurements using either 5-, 2- or 1-parameter modeling for assessing injury-associated changes in spinal cords in squirrel monkeys in order to optimize a rapid, sensitive, and high-resolution PSR mapping protocol for applications in primates at high field. In addition, the sensitivity of PSR to demyelination in the dorsal pathway rostral and caudal to an injury site has been evaluated.

Introduction

Demyelination is a hallmark of the effects of spinal cord injury (SCI), and quantitative magnetization transfer (qMT) MRI provides a noninvasive means to detect and grade myelination after an injury and during repair. This study aims to systematically evaluate the accuracy and precision of estimates of pool size ratio (PSR) from qMT using different modeling approaches in data analyses for monitoring injury-associated changes in the spinal cords of squirrel monkeys. A primary goal is to optimize a rapid, sensitive and high-resolution PSR mapping protocol for assessing SCI in primates at high field.

Methods

MRI scans were performed in anesthetized squirrel monkeys at 9.4T, before and after a unilateral dorsal column lesion of the cervical spinal cord. Quantitative MT data were collected for a coronal slice (Fig. 1), using a 2D MT-weighted spoiled gradient recalled-echo sequence (TR 24 ms, flip angle = 7°, resolution = ~0.313x0.313x1 mm^3, 32 acquisitions). Gaussian-shaped saturation pulses (θ_{sat} = 220° and 820°, pulse width = 12 ms) were used with 12 RF offsets spaced at constant logarithmic intervals between 1 and 100 kHz. Histological sections using myelination stains were obtained post mortem for comparison. MRI data were analyzed using MATLAB. A 5-parameter model,[1] and 2- and 1-parameter models[2] with a reduced number of RF offsets were applied to derive estimates of PSR. 5Pfit derives from 5-parameter fitting using all the qMT data. 2Pfit represents 2-parameter fitting results using only 2-6 RF offsets (defined as 2Pfit(2RF), 2Pfit(3RF), 2Pfit(4RF), 2Pfit(5RF), and 2Pfit(6RF) respectively). Direct 1-parameter measures with different RF offset pairs (one at 100 kHz), are denoted by the other selected RF offset e.g. 820RF4 (~3.5 kHz), 820RF5 (~5.3 kHz), 820RF6 (~8.1 kHz), 820RF7 (~12.3 kHz) and 820RF8 (~18.7 kHz) for data obtained with θ_{sat} 820°, and 220RF1 (1 kHz), 220RF2 (~1.5 kHz), 220RF3 (~2.3 kHz), 220RF4 (~3.5 kHz), and 220RF5 (~5.3 kHz) for data using θ_{sat} 220°. Numerical simulations were also performed to test modeling performance for different approaches and SNR.[3] The regional correlations between PSR from different approaches were calculated using the Pearson correlation function, and it was assumed that 5Pfit was the most accurate method of analysis. The significance of PSR differences was evaluated using Student's t-tests.

Results

The performance of different data analyses was systematically evaluated for the simulated data. Higher SNR and a larger number of RF offsets significantly reduced experimental errors and variance (Fig. 2a). At least 3 RF offsets are required in 2Pfit to retain comparable accuracy and precision as that obtained from 5Pfit with 12 RF offsets (Fig. 2a). The 1-parameter calculation

Figures

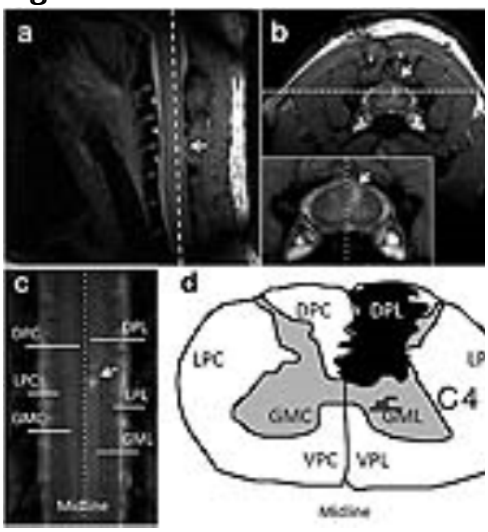

Figure 1. MTC images showing a unilateral dorsal column lesion in squirrel monkey. (a) Sagittal view. (b) Axial view. (c) Coronal view. (d) Schematic illustration of the targeted lesion of unilateral dorsal column (black patch). The arrow indicates the lesion site. White dashed lines indicate the location of a coronal imaging plan. DPC, LPC, VPC and GMC indicate dorsal pathway, lateral pathway, ventral pathway and gray matter (GM) on the control side respectively; DPL, LPL, VPL and GML indicate dorsal pathway, lateral pathway, ventral pathway and GM on the lesion side respectively.

requires higher SNR (more than 1.5 times) to approach comparable accuracy and precision as 5Pfit with 12 RF offsets (Fig. 2a). The 1-parameter calculation is very sensitive to RF offset and power, but the optimum offset and power can be determined. Relative bias in PSR value was estimated for 2-parameter fitting (Fig. 2b). All the selected modeling approaches detected the lesion/cyst as a change in PSR at the site of injury (Fig. 3a). However, the regional contrasts in PSR maps from the different approaches varied, with 2Pfit showing strong positive correlations with 5Pfit (Fig. 3b). The variations from 1-parameter measures were large across RF offsets, powers and sessions at the experimental SNR (~75), and 820RF6 and 220RF3 showed stronger correlations with 5Pfit than measures using other selected RF offsets for 1-parameter modeling (Fig. 3b). Histology confirmed that reduced values of PSR corresponded to demyelination along the dorsal pathway on the injury side (Fig. 4). The rostral side (to the lesion) showed more severe demyelination than the caudal side in the representative injured subjects (Fig. 4). The optimum 2- and 1-parameter approaches were very sensitive in detecting cysts (Fig. 5a), and they also provided comparable sensitivity as 5-parameter modeling to detect regional demyelination and loss of macromolecules around the injury site (Fig. 5a). The decrease of PSR in GM (Fig. 5a) was not as evident as that in the dorsal pathway. The results from 2- or 1-parameter modeling could underestimate PSR of cyst (Fig. 5b), due to the relative bias (Fig. 3b) caused by fixing R_aT_{2a}, T_{2b}, and RM_{0a} when their actual values are very different in cyst.[4]

Conclusions

These results support the use of the optimized 2- or 1-parameter approaches for qMT imaging of injured spinal cord as a means to reduce total imaging time and/or permit additional signal averaging. PSR detected demyelination rostral and caudal to lesions, especially in the dorsal pathway on the lesion side.

Acknowledgements

We thank Mrs. Chaohui Tang and Mr. Fuxue Xin of the Vanderbilt University Institute of Imaging Science for their assistance in animal preparation and care in MRI data collection. This study is supported by DOD grant W81XWH-17-1-0304, and NIH grants NS092961, NS078680, and NS093669.

References

1. Ramani, A., et al., Precise estimate of fundamental in-vivo MT parameters in human brain in clinically feasible times. Magn Reson Imaging, 2002. 20(10): 721-31.

2. Underhill, H.R., et al., Fast bound pool fraction imaging of the in vivo rat brain: Association with myelin content and validation in the C6 glioma model. Neuroimage, 2011. 54(3): 2052-2065.

3. Cercignani, M. and D.C. Alexander, Optimal acquisition schemes for in vivo quantitative magnetization transfer MRI. Magn Reson Med, 2006. 56(4): 803-10.

4. Wang, F., et al., Longitudinal Assessment of Spinal Cord Injuries in Nonhuman Primates with Quantitative Magnetization Transfer. Magn Reson Med, 2016. 75(4): 1685-1696.

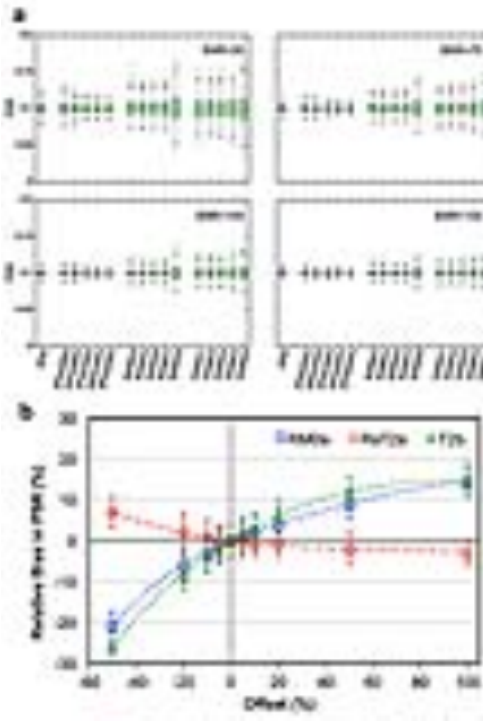

Figure 2. Accuracy and precision of PSR measures. (a) Boxplots of PSR from selected analytic approaches. PSR = 0.1 was used to synthesize qMT data with 12 RF offsets from 1 to 100 kHz at 820° and 220° at different SNR levels, with other parameters adopted from previous study in normal spinal cords.[4] The circles and middle lines represent mean and median values respectively (N=1024). (b) Relative bias in PSR when the actual RM_{0a}, R_aT_{2a} or T_{2b} is different from the fixed reference value in 2-parameter modeling (5 RF offsets). Error bars represent standard deviations (SNR=75, N=1024).

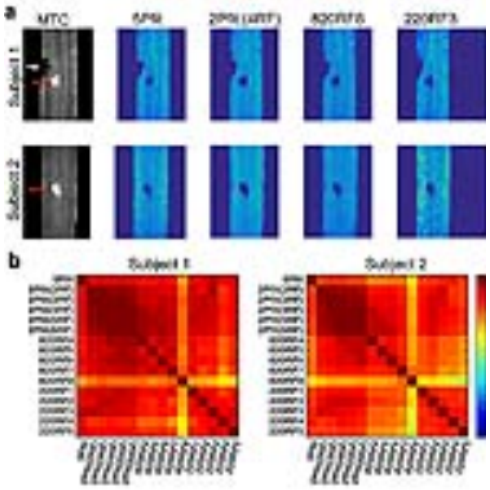

Figure 3. Comparison of PSR of injured spinal cord of squirrel monkey from selected modeling approaches. (a) Selected PSR maps showing 5-parameter fitting (5Pfit) using data with 12 RF offsets, 2-parameter fitting (2Pfit) using data with 4 RF offsets, 1-parameter calculation based on data with RF6 and RF12 at 820° (820RF6), and 1-parameter calculation based on data with RF3 and RF12 at 220° (220RF3). (b) Correlation coefficients between PSR measures from selected modeling approaches ($p < 0.05$ for all). All pixels in the middle 1.5 cm were included in the correlation analysis.

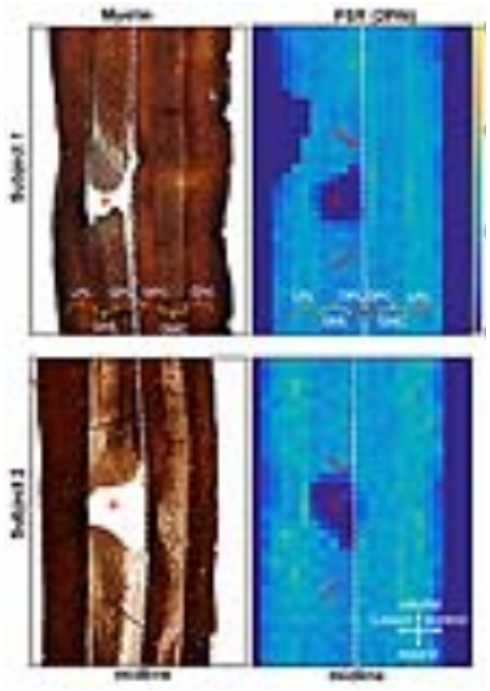

Figure 4. Comparison of PSR maps and corresponding spinal cord tissues with myelin stains. Asterisks indicate lesion/cyst site, and red arrows indicate the unilateral demyelination in the dorsal pathway on the lesion side, both caudal and rostral to the lesion site. PSR maps from 2-parameter fitting using 4 RF offsets are shown for comparison. DPC, LPC, and GMC indicate dorsal pathway, lateral pathway, and GM on the control side respectively; DPL, LPL, and GML indicate dorsal pathway, lateral pathway, and GM on the lesion side respectively.

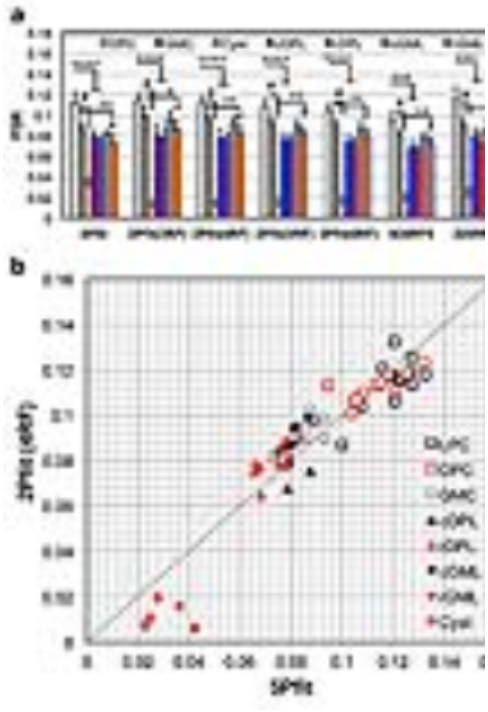

Figure 5. Comparison of regional PSR of injured spinal cord across subjects (N=12 for the control, N=5 for the injured). (a) The regional averaged PSR across subjects from selected modeling approaches. The bars represent standard deviations. DPC and GMC indicate dorsal pathway and GM on the control, while rDPL, cDPL, rGML, and cGML indicate rostral dorsal pathway, caudal dorsal pathway, rostral GM, and caudal GM on the lesion side of the injured subjects, respectively. (b) The comparison between 5-parameter and 2-parameter modeling, and 2Pfit

(4RF) was shown. *p<0.05, **p<5x10^{-3}, ***p<1x10^{-4}, ****p<1x10^{-5}, and #p<1x10^{-6}.

1119

Validation of spinal cord fMRI with LFP and spike activity in non-human primates

Tung-Lin Wu[1,2], Pai-Feng Yang[1,3], Feng Wang[1,3], Zhaoyue Shi[1,2], Arabinda Mishra[1,3], Ruiqi Wu[1], Li Min Chen[1,3], and John C Gore[1,2,3]

[1]Vanderbilt University Institute of Imaging Science, Nashville, TN, United States, [2]Biomedical Engineering, Vanderbilt University, Nashville, TN, United States, [3]Radiology and Radiological Sciences, Vanderbilt University Medical Center, Nashville, TN, United States

Synopsis

Stimulus-driven and resting-state fMRI BOLD signals have previously been reported in the spinal cord to delineate its functional architecture. However, validation of these resting-state findings has yet to be performed. In this study, we compared spinal fMRI results with electrophysiology (LFP and spike activity) in non-human primates and found that 1) signals elicited by stimulation occur predominantly in the ipsilateral dorsal horn and only in the appropriate segments 2) resting-state dorsal-dorsal functional connectivity is significantly greater than that in dorsal-to-intermediate-gray-matter, and 3) resting-state functional connectivity is spatially constrained to two spinal segments.

Background

To date, the functional organization of the spinal cord (SC) remains relatively unexplored compared to the brain despite its importance serving as a conduit for motor outputs from the brain, peripheral inputs to the brain and as a center for coordinating certain reflexes. This is partly due to its small physical size and the presence of pronounced physiological noise and distortions from magnetic field inhomogeneities [1]. Stimulus-driven fMRI has been reported for over a decade [2], but only recently have resting-state networks within cord grey matter been reliably found in both humans and animals [3]–[5]. Specifically, dorsal-dorsal and ventral-ventral resting-state BOLD correlations have been shown to be significantly more robust when compared to connectivity between other pairs of regions (horns). However, validation of these resting-state findings has yet to be performed. Thus in this study, we combined measurements of local field potentials (LFPs) and spiking activity in non-human primates (NHPs) to validate findings from stimulus-driven and resting-state fMRI.

Methods

Eight adult male squirrel monkeys were included in this study. Four animals underwent laminectomy and subsequent electrophysiology recordings. Resting-state and stimulus-driven (8Hz innocuous tactile, 30s on/off, 10 epochs) MRI acquisitions were obtained on a 9.4T Varian magnet with a saddle-shaped transmit-receive surface coil. Five anatomic axial images were obtained using magnetization transfer contrast (TR/TE=220/3.24ms, 0.25x0.25x3mm^3) while BOLD images were acquired using a fast gradient echo sequence (TR/TE=46.9/6.50ms, 0.5x0.5x3mm3). Previously acquired spinal fMRI datasets with a higher temporal resolution (TR=24.0ms) on healthy monkeys were also included in group analyses. Data pre-processing and ROI analysis procedures were standard and were described in our previous publication [3].

A four-shank linear microelectrode-array (Microprobes Blackrock, 16 channels/shank, 150m separation between contacts) covering various depths was used to collect resting-state (15 minutes) and stimulus-evoked (same paradigm design as MRI) recordings; 2-3 runs were collected for each monkey. LFP signals were sampled at 500Hz, notch-filtered at 60 and 120Hz, and 1-150Hz band-pass filtered. Stimulus-driven LFP data were separated into stimulus-on and stimulus-off periods before power differences were computed at the first five harmonics of 8Hz from Welch's power spectra. Spike activity events were evaluated with rate histograms, raster plots and peri-event histograms. Resting-state LFPs were further de-noised by notch-filtering the first five harmonics of the respiration frequency. Using channels with greatest LFP responses as seeds, resting-state coherences were computed between dorsal horns within and across slices. As controls, coherences between dorsal horns and dorsal-to-intermediate-gray-matter were computed as well.

Results and Discussion

Figures

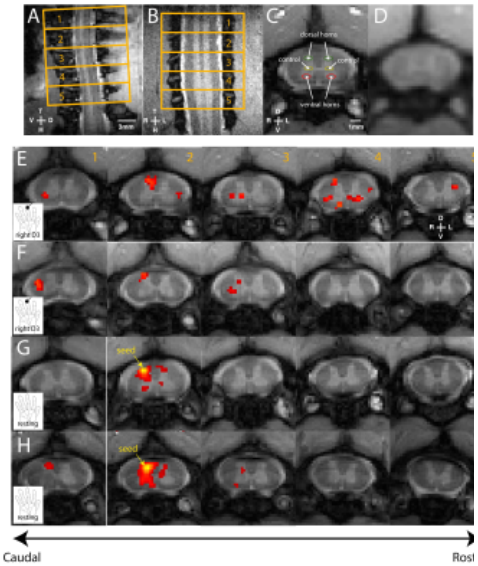

Stimulus-driven and resting-state fMRI in non-human primates at 9.4T. (A) Sagittal and (B) coronal views of the spinal cord in magnetization transfer contrast (MTC) images. (C) MTC and (D) BOLD axial images. Red and green circles indicate dorsal and ventral horns respectively. Yellow circles present intermediate gray matter of the spinal cord used as controls for later quantifications. (E-F) Activation maps to D3 tactile stimulation, and (G-H) resting-state connectivity patterns of seeds in the dorsal horns. Results presented here are from the four monkeys that underwent electrophysiological recordings. D, dorsal; V, ventral; R, rostral; C, caudal; H, head; T, tail.

We first reproduced fMRI findings from our previous publications in the four monkeys that underwent electrophysiology (Figure 1): innocuous tactile stimulation elicited strongest signal on the ipsilateral dorsal horn, while within-slice resting state dorsal-dorsal connections were most prominent compared to control regions. Spinal segments for different digits were identified with electrophysiology recordings, based on neurons' receptive field properties (Figure 2). Targeted recordings at two spinal segments further confirmed neuronal origins of activity evoked by tactile stimuli used in fMRI studies. Specifically, robust LFP activations are evident as synchronous voltage changes with the stimulus paradigm (yellow shades in Figure 3E-H) along with apparent frequency peaks at 8Hz harmonics in the power spectra (Figure 3I-L). Similarly, spike histograms show significantly greater spike rates during stimulus-on while peri-event rasters present consistent firing of neuronal discharges with the stimulus external event (Figure 3M-T). Figure 3A-D presents averaged power changes for stimulation of different digits, and Figure 4 overlays averaged LFP, spike rate and fMRI in one representative monkey, SQM-3815. Overall, significant power changes were observed in the ipsilateral dorsal horn of the appropriate cervical segment, a finding that is congruent with previously reported fMRI studies [2,3].

Inter-horn resting-state connectivity patterns observed in fMRI were also validated using LFP coherences (Figure 5). Specifically, within-slice dorsal-dorsal functional connectivity was stronger than in dorsal-to-intermediate-gray-matter for both fMRI and LFP. Moreover, across-segment dorsal-to-dorsal connectivity was significantly weaker than that within-slice, an observation consistent with the bell-shaped correlation profile found in fMRI [3]. Trends of connectivity measures in different ROI pairs were also highly similar between the two (r=0.94, p=0.057) while Bonferonni corrected Mann-Whitney tests between different ROI selections support this observation. Overall, we have validated previously reported fMRI findings in spinal cords with direct invasive measurements of neuronal activity in NHPs.

Conclusion

High agreements between fMRI and electrophysiology findings imply that fMRI can be reliably used to assess functional circuits in the SC and are most likely reflective of neuronal activity. Both modalities point to parallel conclusions, and findings here may lay the foundation to assessing and monitoring SC injuries in patients by using resting-state fMRI.

Acknowledgements

We thank Mrs. Chaohui Tang and Mr. George H. Wilson of the Vanderbilt University Institute of Imaging Science for their assistance in animal preparation and data collection.

References

[1] F. Eippert, Y. Kong, M. Jenkinson, I. Tracey, and J. C. W. Brooks, "Denoising spinal cord fMRI data: Approaches to acquisition and analysis.," Neuroimage, 2016.

[2] P. W. Stroman, "Magnetic Resonance Imaging of Neuronal Function in the Spinal Cord: Spinal fMRI," Clin. Med. Res., vol. 3, no. 3, pp. 146–156, 2005.

[3] L. M. Chen, A. Mishra, P.-F. Yang, F. Wang, and J. C. Gore, "Injury alters intrinsic functional connectivity within the primate spinal cord.," Proc. Natl. Acad. Sci. U. S. A., vol. 112, no. 19, pp. 5991–6, 2015.

[4] R. L. Barry, S. A. Smith, A. N. Dula, and J. C. Gore, "Resting state functional connectivity in the human spinal cord," Elife, vol. 2014, no. 3, pp. 1–15, 2014.

[5] T.-L. Wu, F. Wang, A. Mishra, G. H. Wilson, N. Byun, L. M. Chen, and J. C. Gore, "Resting-state functional connectivity in the rat cervical spinal cord at 9.4 T," Magn. Reson. Med., Sep. 2017.

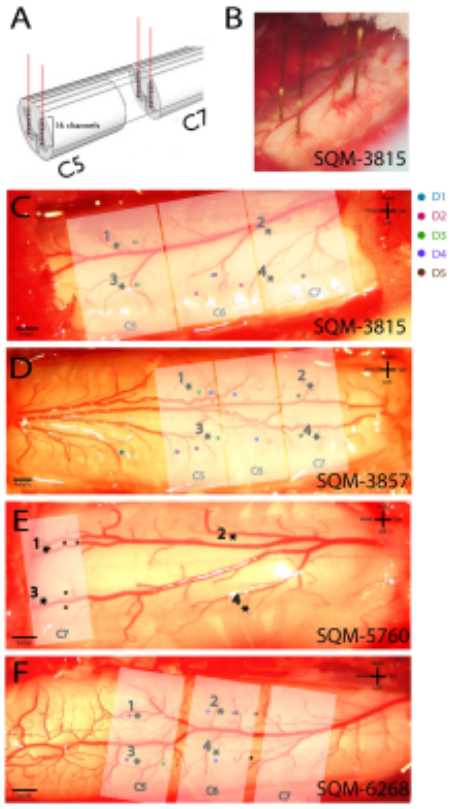

Electrophysiological recording setup, recording sites and maps of different digits segments for the four squirrel monkeys (SQMs). (A) Schematic diagram of the spinal cord inserted with four electrodes, each with 16 channels that are 150 apart. (B) Sample photograph of the four inserted electrodes in SQM-3815. Exposed spinal cord with mapped digit regions (color dots) and recording sites (black asterisks) for (C) SQM-3815, (D) SQM-3857, (E) SQM-5760 and (F) SQM-6268. Shaded white regions are estimated segments of the spinal cord.

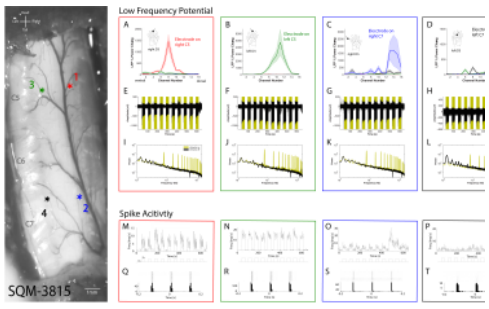

Stimulus-driven LFP and spike activity in one representative

monkey, SQM-3815. (A-D) LFP power changes computed from Welch's power spectra between 30s stimulus-on and -off in all four electrodes under right-D3, left D3, right-D5, and left-D5 innocuous 8Hz tactile stimulus conditions respectively. (E-H) LFP time series from the channel that presents the greatest power change and its respective (I-L) Welch's power spectra. (M-P) Spike rate histograms at the channels corresponding to largest LFP power changes and their corresponding (Q-T) raster plots (top row) and peri-event histograms (bottom row) for the digit stimulation conditions.

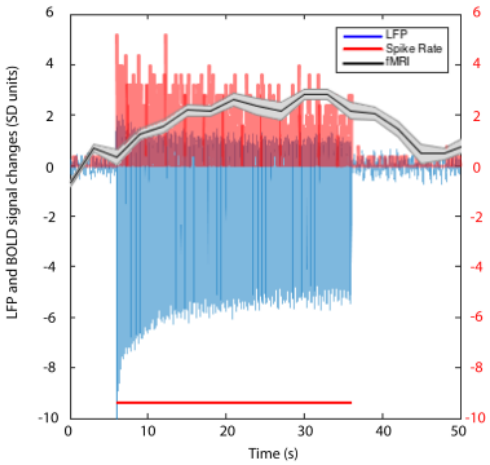

Responses to innocuous tactile stimulation. Overlay of averaged fMRI (black), LFP (blue) and spiking activity (red) in the ipsilateral dorsal horn of the appropriate segment elicited by innocuous 8Hz tactile stimulation from SQM-3815. Red horizontal line at the bottom of the plot represents onset of the stimulation. Spike rate histograms were computed at a bin size of 0.05s, and results are plotted in units of standard deviation (SD).

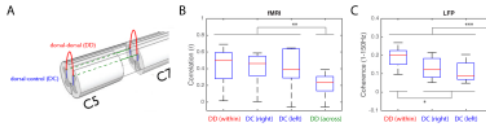

Comparison between resting-state fMRI and LFP connectivities. (A) Schematic diagram of coherences computed in the

recordings of the spinal cord. Within and across dorsal to dorsal (DD) as well as dorsal to control (DC) connectivities were computed; control region is identified as intermediate gray matter of the spinal cord. (B) Group boxplots of within and across DD, and DC right and left connectivity measures are displayed as (B) Pearson's correlation for fMRI and (C) averaged coherences for LFP. *p<0.05, **p<0.01, and ***p<0.005 Bonferonni corrected Mann-Whitney Test.

Validation of Structural, Molecular, and Functional Imaging Biomarkers

SC160154 Spinal Cord Injury Research Program
W81XWH-17-1-0304

PI: John C. Gore **Org:** Vanderbilt University Medical Center **Award Amount:** $783,554

Study/Product Aim(s)

- Determine how the functional integrity of injured spinal cord grey matter repairs over time using functional MRI.
- Determine how injured spinal cord white matter repairs over time using structural and molecular MRI.
- Validate our MRI findings with invasive, gold-standard measures. These will include electrophysiology, behavioral measures and quantitative analyses of histological sections obtained at different time points during the course of recovery.

Approach

•We will implement sub-millimeter fMRI and multiparametric MRI (CEST, qMT, DTI) at 9.4 Tesla with optimized acquisition sequences and post-processing algorithms to measure functional connectivity, molecular changes, and structural alterations in normal spinal cord and after spinal cord injury and recovery in non-human primates (NHP). fMRI/MRI will be validated with electrophysiology, behavior, and histology.

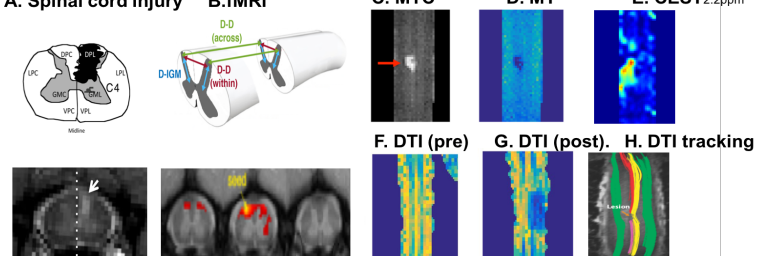

Spinal cord MRI biomarker research. (A) Unilateral injury (top schematic, injury in black; bottom MRI, arrow) and recovery assessed via (B) functional connectivity within/across slices (top schematic, bottom fMRI). (C) MTC detects injury (arrow), quantified by (D) MT, (E) CEST, (F, G) DTI (FA pre and post injury) & (H) fiber tracking.

Accomplishments:
We refined and validated with electrophysiology BOLD and resting state fMRI.
Structural and molecular MRI (MT, CEST, DTI) were refined and data acquired.
FMRI/MRI were implemented in spinal cord injury, validated with histology, in NHPs.

Timeline and Cost

Activities CY	17	18	19	20
fMRI/MRI in NHPs; implement in first cohort of SCI NHPs with validation.				
Implement and validate methods in SCI.				
Implement and validate methods in SCI; identify sensitive biomarkers.				
Estimated Budget $783,554	**$267995**	**$272006**	**$243553**	

Updated: Nashville, TN, USA July 15, 2018

Goals/Milestones

CY17 Goal – Refinement of spinal cord (SC) fMR/MRI methods; implementation and validation in first SC injury (SCI) cohort

☑Implement fMRI/MRI on NHP, validate with electrophysiology.

❑Implement fMRI/MRI in SCI; validate (recordings, histology).

CY18 Goals – Implementation and validation of SCI recovery

☐ Implement fMRI/MRI in SCI and follow recovery over a 6 month period; validate (recordings, histology).

CY19 Goal –Implementation and validation of SCI recovery

☐ Implement fMRI/MRI in SCI and follow recovery over a 6 month period; validate (recordings, histology).

☐ Identify biomarkers most sensitive to SC injury and recovery.

Comments/Challenges/Issues/Concerns

- Delay in ACURO and local IACUC approval until Sept. 16, 2018.

Budget Expenditure to Date

Projected Expenditure: $267,995
Actual Expenditure: $255,443